J Nanopart Res (2011) 13:127–138
DOI 10.1007/s11051-010-0010-7

RESEARCH PAPER

Microwave-assisted polyol synthesis of Cu nanoparticles

M. Blosi · S. Albonetti · M. Dondi · C. Martelli · G. Baldi

Received: 9 February 2010 / Accepted: 21 June 2010 / Published online: 14 July 2010

Abstract Microwave heating was applied to synthesize copper colloidal nanoparticles by a polyol method that exploits the chelating and reducing power of a polidentate alcohol (diethylenglycol). The synthesis was carried out in the presence of eco-friendly additives such as ascorbic acid (reducing agent) and polyvinylpirrolidone (chelating polymer) to improve the reduction kinetics and sols stability. Prepared suspensions, obtained with very high reaction yield, were stable for months in spite of the high metal concentration. In order to optimize suspensions, synthesis parameters were modified and the effects on particle size, optical properties, and reaction yield were investigated. XRD analysis, scanning transmission electron microscopy (STEM), and DLS measurements confirmed that prepared sols consist of crystalline metallic copper with a diameter ranging from 45 to 130 nm. Surface plasmon resonance (SPR) of Cu nanoparticles was monitored by UV–Vis spectroscopy and showed both a red shift and a band weakening due to nanoparticle diameter increase. Microwave use provides rapid, uniform heating of reagents and solvent, while accelerating the reduction of metal precursors and the nucleation of metal clusters, resulting in monodispersed nanostructures. The proposed microwave-assisted synthesis, also usable in large-scale continuous production, makes process intensification possible.

Keywords Copper · Nanoparticles · Colloid · Polyol synthesis · Microwave

M. Blosi (✉) · M. Dondi
ISTEC-CNR, Institute of Science and Technology for Ceramics, CNR, National Research Council, Via Granarolo 64, 48018 Faenza, Italy
e-mail: magda.blosi@istec.cnr.it

M. Dondi
e-mail: michele.dondi@istec.cnr.it

S. Albonetti
Department of Industrial Chemistry and Materials, INSTM, Research Unit of Bologna, University of Bologna, Viale Risorgimento 4, 40136 Bologna, Italy
e-mail: stalbone@ms.fci.unibo.it

C. Martelli
Department of Industrial Chemistry and Materials, University of Bologna, Viale Risorgimento 4, 40136 Bologna, Italy

G. Baldi
CERICOL, Colorobbia Research, Via Pietramarina 123, 50053 Sovigliana Vinci, Italy
e-mail: baldig@colorobbia.it

Introduction

In recent years, great interest has been devoted to the synthesis of metal nanoparticles in order to explore their special properties and potential applications. It is mainly noble metals, due to their optical, catalytic, and thermal properties, that are being exploited

(Lu et al. 2009; Zheng et al. 2007; Dotzauer et al. 2009; Singh and Raykar 2008) despite their costliness. Among them, copper nanoparticles represent an ideal compromise between cost and interesting properties, becoming an industrially important material. In fact, they are widely studied for applications in different fields, such as optical (Tanabe 2007) and magnetic devices (Gritaonandia et al. 2008), in catalysis (Son et al. 2004; Sarkar et al. 2008; Haq and Raval 2007), environmental remediation (Liu et al. 2007), as antibacterial agents (Kim et al. 2006a), or in heat exchangers (Liu et al. 2006; Nada et al. 2008). In fact, an innovative technique for improving heat transfer entails using ultra-fine solid particles dispersed in the base fluids; nanoparticles prevent the sedimentation.

Moreover, copper nanoparticles in the colloidal form, i.e., nanofluids, have many new applications and advantages. For example, due to their extraordinary thermal conductivity, they have recently proved to be of great interest as better coolants than conventional particles (microscale), as they avoid any increase in pressure drop in the flow field (Daungthongsuk and Wongwises 2007). Furthermore, copper nanofluids are also being studied as an antifriction liquid in motor oil that permits less wear among motor metal components (Yu et al. 2008), although the lubricating power could be assured only by a perfect particle dispersion. A key point is the availability of nanoparticles in the colloidal form, which are technologically highly significant, because they improve the industrial scale-up process, by permitting the use of continuous flow systems and guaranteeing the safety of work environments.

For the preparation of copper nanoparticles, several synthesis routes have been described, such as precipitation (Zhu et al. 2004a), thermal decomposition (Kim et al. 2006b), microemulsion (Lisiecki and Pileni 1993), surfactants solution (Wu and Chen 2004), reduction in alcoholic medium (Nakamura et al. 2007; Park et al. 2007), microwave-assisted techniques (Nakamura et al. 2007; Zhu et al. 2005), and vacuum vapor deposition (Liu and Bando 2003). However, most articles involve the precipitation of solids (Cha et al. 2006; Zhao et al. 2004; Zhu et al. 2004b, 2005; Fievet et al. 1993; Wu et al. 2006; Sun et al. 2005; Yang et al. 2006). Only a few reports have focused on the achievement of stable nanosuspensions (Huang et al. 1997; Sidorov et al. 1999) and, even if a small number deal with high solid content, essential for large-scale production (Wu and Chen 2004; Ren et al. 2005; Kobayashi et al. 2009), no environment-friendly reagents are used.

The one-step synthesis approach is particularly important for obtaining suspensions involving particle nucleation directly into the fluid, while avoiding particle separation and re-dispersion steps; it also ensures a better control over particle dispersion and size. The fact of dealing constantly with suspensions represents an essential process goal for the development of large-scale production.

Among the one-step synthesis methods, polyol-mediated synthesis, developed to prepare nanosized metal and alloy particles, allows an accurate and reproducible control of the mean diameter of the particles in a broad size range and the mixing of the reactants at the molecular level (Fievet 2000). In this procedure, "polyol" stands for polyalcohols with a high boiling temperature, which are able to dissolve inorganic salts. For metal nanoparticle preparation, the polyol method was applied because of its moderate reducing properties and also for its chelating effect which avoids the agglomeration of particles during the synthesis. Preparation of mono- or polymetallic particles of cobalt, nickel, copper, and noble metals in the submicrometer and nanometer size range has been reported (Viau et al. 2001; Chakroune et al. 2003; Wang et al. 2006; Zhu et al. 2004b). Recently, this method has received considerable attention because of its simplicity and the advantage, over most other methods, of preparing high-purity metals, oxides, and a variety of other materials (Feldmann and Jungk 2001; Feldmann and Jungk 2002; Hammarberg et al. 2009).

A novel microwave-assisted polyol synthesis of copper nanosuspensions is described here: this method has been developed by evaluating the influence of different synthesis parameters on the suspension features, while focusing particularly on the process aspects, which are essential for the scale-up to a continuous microwave flow system, suitable for large-scale production. Since suspension stability—although rarely dealt with by the literature on copper nanoparticles—represents a key point for the industrial scale-up, we aim to obtain stable Cu nanosuspensions, also by improving the colloidal stability over time.

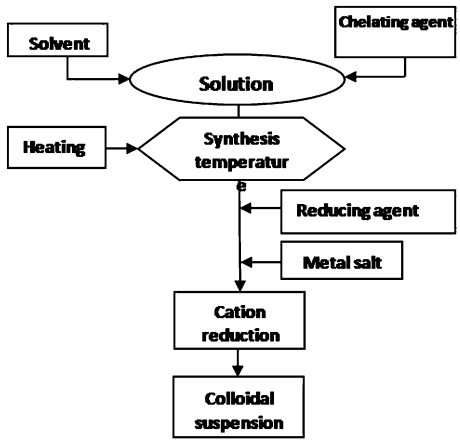

Scheme 1 Reaction flowchart

Experimental

Preparation of nanoparticles

All the chemical reagents used in this experiment were analytical grade (Sigma-Aldrich).

The typical synthesis procedure is illustrated in Scheme 1. First, the chelating agent (polyvinylpirrolidone, PVP K30, Mw 55000) was completely dissolved in 105 mL of diethyleglycol (DEG), and this solution was heated to the synthesis temperature in a microwave oven under magnetic stirring. Once the synthesis temperature was reached, two DEG solutions, containing the proper quantities of either the reducing agent (35 mL of $C_6H_8O_6$ solution) or the metal precursor (20 mL of $Cu(ac)_2{\cdot}H_2O$ solution), were added to the hot PVP solution; the reducing agent solution was poured first, followed by the metal ion solution a few minutes later.

After $Cu(ac)_2$ addition, the green solution turned dark red, thus indicating the immediate nucleation of metallic copper particles. The PVP amount was kept for all samples at a molar ratio of 5 between PVP repetitive units and metal, while, to study the influence of temperature, the heat treatment was performed in the 60–170 °C temperature range. Particular attention was paid to the study of the ascorbic acid and copper acetate addition into the initial PVP solution, because process parameters such as addition order and temperature proved to be key points for the industrial scale-up. In particular, the effect of both the order and the temperature at which the reagents (ascorbic acid and copper acetate) were added into the solution, before or after heating started, was carefully evaluated. The synthesis conditions used for producing the different Cu particles are summarized in Table 1. All the obtained suspensions did not evidence any precipitation until several weeks later.

In addition, in order to evidence the effect of microwave irradiation on the formation of copper nanoparticles, some syntheses were carried out under the same reaction conditions (samples H-t and H2-t),

Table 1 Synthesis conditions for the preparation of Cu particles

Sample	T (°C)	[Cu^{2+}] (mM)	[Cu] (%wt)	S^a	∅DLS (nm)	SD (nm)	PDI	Reaction yield (%)
A	200	16.6	0.09	\	154	±6	0.20	94
B	170	16.6	0.09	2.5	133	±5	0.08	100
Reducing agent effect								
C	170	33.2	0.18	1	238	±8	0.11	95
D	170	33.2	0.18	2.5	130	±5	0.06	100
E	170	33.2	0.18	5	155	±2	0.10	100
F	170	33.2	0.18	15	176	±4	0.10	100
D2	170	33.2	0.18	2.5	215	±15	0.20	–
Temperature effect								
G	140	16.6	0.09	2.5	105	±2	0.06	100
H	100	16.6	0.09	2.5	90	±2	0.03	100
I	60	16.6	0.09	2.5	111	±4	0.07	100

For each sample the ratio [nPVP/$n$$Cu(ac)_2$] was kept at 5. Time synthesis is 10 min except for sample A synthesized for 50 min. Sample D2 was synthesized as sample D, but exchanging the injection order of the reagents ($C_6H_8O_6$ and $Cu(ac)_2$)

[a] Ascorbic acid to metal ion molar ratio

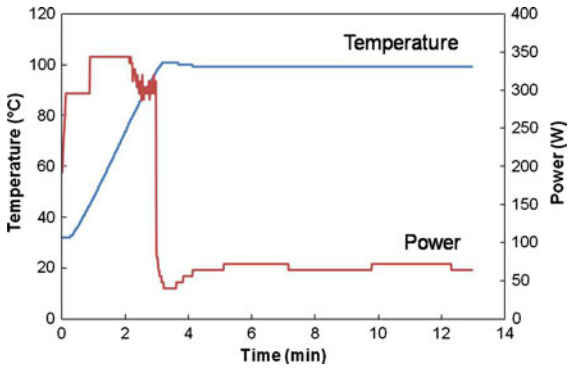

Fig. 1 Temperature and output power profile during microwave heating to 100 °C

but using conventional laboratory heating systems (without using microwave irradiation).

Apparatus

The microwave system used is a Milestone MicroSYNTHplus, whose reaction chamber is fitted with magnetic stirring, reflux system, and an optical fiber temperature controller. The microwave power is generated by 2 × 800 W magnetrons, with frequency 2.45 GHz. In order to respect the scheduled heating ramps, the power is continuously supplied and automatically modulated by a software program; for each ramp only the maximum deliverable power can be imposed. The power is automatically changed by the instrument in order to follow the temperature profile; Fig. 1 shows a typical temperature and output power profile for a reaction at 100 °C.

Analytical characterization

Copper nanosuspensions were characterized by optical spectroscopy (UV–Vis), dynamic light scattering (DLS), X-ray diffraction (XRD), inductively coupled plasma-atomic emission spectrometry (ICP-AES), and scanning transmission electron microscopy (STEM).

UV–Vis extinction spectra were measured with a Lambda 35 spectrophotometer (Perkin Elmer, UK), using a quartz cuvette as sample-holder. Samples were prepared by diluting the as-prepared colloidal suspension with DEG in order to have the same metal concentration for every sample.

Particle size distribution, based on hydrodynamic diameter, was evaluated by a nanometric particle size analyzer, Zetasizer Nano S (Malvern Instruments, UK); scattering data were recorded at 25 ± 1 °C in backscattering modus at a scattering angle of $2\theta = 173°$. Before measurement, samples were properly diluted with DEG. Each result corresponds to the average of five measurements, and each measurement is averaged within 15 performed analyses. Hydrodynamic diameter includes the coordination sphere and the species adsorbed on the particle surface such as stabilizers, surfactants, and so forth. DLS analysis provides also a polydispersion index (PDI), ranging from 0 to 1, to quantify the colloidal dispersion degree; for PDI lower than 0.2 samples may be considered monodispersed. Prepared samples show a narrow, Gaussian-type particle size distribution (PDI $\leq$0.2).

Diffraction patterns were collected on the synthesized samples dripped onto a glass slide and dried at 100 °C in air atmosphere for 2 h. Analyses were performed by a D500 diffractometer (Siemens, Germany) operating with Ni-filtered Cu Kα radiation (35–52° 2θ range, 0.02 s^{-1}, 3 s time-per-step).

Unreacted metal cations were detected by ICP-AES in order to determine the reaction yield. Samples were prepared as follows: 50 mL of synthesized colloid was poured into a semi-permeable osmotic membrane (Visking tube), which was submerged in a de-ionized water bath. Osmotic pressure caused the exchange of unreacted cations into the external water and the water entry into the tube. After 1 h, the equilibrium was attained and the external liquid underwent ICP (Liberty 200, Varian, Australia) quantitative analyses (Cu line 324.754 Å, plasma power 1.20 kW, plasma flow 15 L min^{-1}, sample pump rate 15 rpm).

Particles were observed under a field emission scanning electron microscope (FESEM, Supra 40, Zeiss, Germany) equipped with an electron detector unit working in a transmission mode (GEMINI® multi mode STEM detection system, Zeiss, Germany) that provides images, similar to TEM analysis, collected at 20 kV. Specimens were prepared by dropping the colloidal suspensions, previously diluted in water (1:300), onto a metal grid coated with a polymer film. Drops were evaporated at room temperature in ambient atmosphere. Average particle size, standard deviation, and percentage shown in the histogram were calculated on more than 100 particles, by analyzing different images.

Table 2 Samples synthesized at 100 °C by changing the reagents injection temperature: 100 °C (after heating ramp) and 25 °C (before heating ramp)

Sample	Reagents injection temperature (°C)	∅DLS (nm)	SD (nm)	PDI	Instability index (Δnm/day)
H	100	90	±2	0.07	9
H2	25	84	±1	0.08	0
H-t	100	85	±2	0.17	3
H2-t	25	130	±3	0.12	1

Samples H-t and H2-t were prepared using a traditional heating system

Results and discussion

Stable copper nanosuspensions were synthesized by a microwave-assisted polyol route and, in order to improve the system, both synthesis and process parameters were evaluated. Table 1 lists the samples prepared by varying synthesis parameters (metal ion concentration, reducing agent amount, and synthesis temperature), while Table 2 reports the samples obtained by changing some process parameters, such as the reagents' injection temperature or heating mode. Sample A was prepared via polyol-mediated route as reported by Zhao et al. (2004), but adding PVP as chelating agent and replacing ethylenglycol (EG) with diethylenglycol (DEG). In fact DEG, due to its molecular structure, provides a better chelating action, and its higher boiling point (245 °C) makes it possible to avoid an excessive bubble formation.

In this first reaction, the synthesis was carried out by dissolving the metal salt, copper acetate, in DEG; then, in order to maximize the reducing power of DEG, the mixture was rapidly heated to 200 °C by microwave irradiation. After 50 min the precipitation of the metal occurred. During this step, the surface of the growing particles was complexed by DEG as a chelating agent, thus preventing particle growth and aggregation. However, in order to further improve the colloidal stability, PVP was also added.

Figure 2a shows the different steps in the Cu^{2+} reduction during this synthesis. These phases are clearly observed, due to the slow reaction rate. At first, the precursor solution was green in color, a typical feature of copper acetate, with a weak UV–Vis absorption peak at 725 nm; then, after 30 min, a peak appeared at 450 nm (Fig. 2b), corresponding to the formation of the yellow intermediate state, Cu_2O

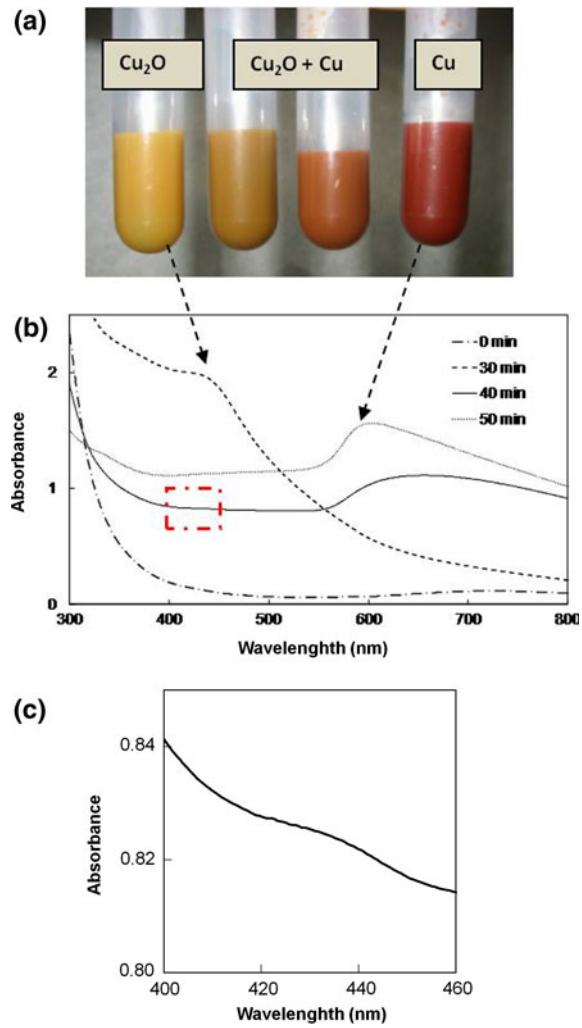

Fig. 2 **a** Color changes indicating the reaction advancement. **b** UV–Vis absorbance spectra corresponding to different reaction stages; SPR bands of Cu^0 and of Cu_2O are indicated by the *arrows*. **c** Enlargement of the part of spectra corresponding to the peak of Cu_2O in the sample collected at 40 min

(Zhao et al. 2004). Lastly, some intermediate states corresponding to a mixture of metal and oxide were detected, and after 50 min the suspensions acquired the characteristic red copper color and the extinction spectrum typical of copper nanoparticles (Lisiecki et al. 1996; Yeh et al. 1999; Creighton and Eadont 1991) was detected at approximately 590 nm (Khanna et al. 2009).

Reducing agent influence

The preparation of sample A presented a series of disadvantages, such as the high temperature (200 °C) needed to guarantee the right polyol reducing power, together with a very long reaction time (50 min); therefore, the following syntheses were performed by adding ascorbic acid as the reducing agent, in order to increase the reducing rate at lower temperatures also. The first test (sample B) indicated that the introduction of the reducing agent was fundamental for improving the reaction. In fact, thanks to the fast reduction induced by ascorbic acid, the synthesis temperature dropped from 200 to 170 °C, and the reaction time from 50 to 10 min, thus resulting in a decrease both in the particle size, from 154 to 133 nm (Table 1), and in the PDI, from 0.2 to 0.08. Furthermore, while sample A after 2 weeks exhibited the formation of precipitate and a solution color shift from red to blue-greenish (typical of Cu^{2+} cation), sample B showed a colloidal stability of about 2 months, without any color change. In fact, ascorbic acid, providing an antioxidant effect (Wu et al. 2006), also improved the colloidal stability. This key role of the ascorbic acid addition can be explained by the fact that the precursor reduction rate is strictly linked to the following metal nanoparticle nucleation and growth processes. The introduction of ascorbic acid greatly increases the reduction rate, by inducing a rapid and massive nucleation and leading to small particle dimensions and homogeneous particle size distribution.

On the basis of these results, the amount of reducing agent, expressed as ascorbic acid to metal molar ratio (S), was optimized. Table 1 lists the samples prepared at 170 °C for different S values; it can be seen that for the two concentrations used (16.6 and 33.2 mM) both particle size and PDI decreased for $S = 2.5$, corresponding to a dynamic equilibrium between reduction, nucleation, and growth, as

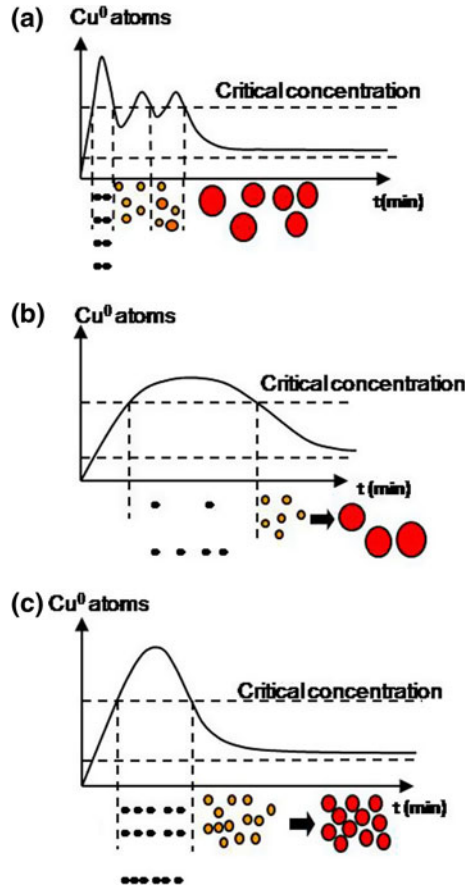

Fig. 3 Nucleation and growth schemes: **a** nucleation speed too high, multistep nucleation, **b** nucleation speed too low, **c** optimized experimental conditions: nucleation and growth equilibrium

described by the scheme (Fig. 3) inspired by LaMer's theory on particle nucleation (LaMer and Dinegar 1950). In fact, if the reduction rate is too slow, such as in sample A, free of ascorbic acid, or sample C, with a sub-stoichiometric S value, only a few nuclei are generated and the growth step is enhanced, resulting in a particle size increase (Fig. 3b). Likewise, particle dimensions also increase if the reduction rate is too fast, as in sample F, which shows a large ascorbic acid excess, because numerous nuclei are formed and nucleation occurs in both multiple-step dissolution and crystallization phenomena (Fig. 3a).

The reaction yields were very high for all samples (Table 1); nevertheless, the reaction completion was achieved only for samples with an S ratio higher than 2.5, even at the lowest synthesis temperature (sample I).

Reaction yield represents a key point for large-scale production in order to both optimize the process and know the actual suspension solid content.

Influence of synthesis temperature

The role of temperature on nucleation and growth phenomena was investigated by synthesis at temperatures ranging from 60 to 170 °C, while keeping the copper concentration (16.6 mM) and ascorbic acid to metal ion ratio (2.5) constant (Table 1).

On the basis of DLS, sample H (Fig. 4), synthesized at 100 °C, shows the smallest particle diameter, because at this temperature a dynamic equilibrium between nucleation and growth was reached (Fig. 3c). Otherwise, low synthesis temperatures drove the system toward a situation of poor nuclei formation, followed by a progressive and constant growth (Fig. 3b), while higher temperatures induced a strong nucleation that developed through a multistep process with a subsequent excessive particle growth (Fig. 3a).

The optical spectra of copper samples, achieved at different synthesis temperatures, exhibit a strong absorption in the visible region, called surface plasmon resonance (SPR). Surface plasmons (SPs) are charge-density oscillations confined to metal nanoparticles. The excitation of SP by an electric field at an incident wavelength, where resonance occurs, results in strong light scattering, the appearance of intense SP absorption bands, and the enhancement of local electromagnetic fields. The

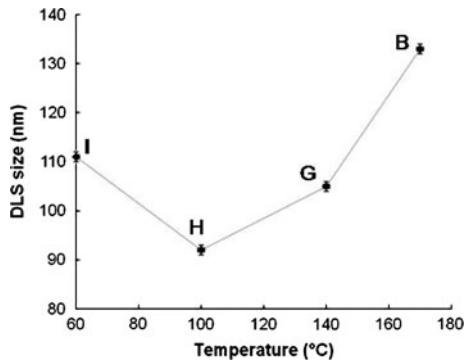

Fig. 4 Particle size (by DLS) of samples achieved with different synthesis temperatures. Time reaction 10 min, concentrations of metal ions: 16.6 mM, $[n\text{PVP}/n\text{Cu}^{2+}] = 5$ and $[n\text{C}_6\text{H}_8\text{O}_6/n\text{Cu(ac)}_2] = 2.5$

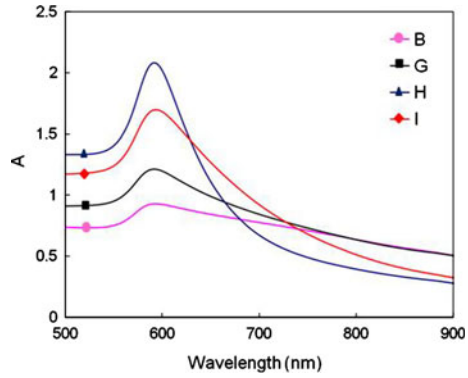

Fig. 5 UV–Vis spectra of samples obtained at different synthesis temperatures: B (170 °C), G (140 °C), H (100 °C), I (60 °C)

frequency (i.e., absorption maxima or color) and intensity of SPR absorption bands are characteristic of the type of material and are highly sensitive to the size and shape of the nanostructures as well as to their surrounding environments (Hutter and Fendler 2004; Lisiecki et al. 1996; Kreibig and Genzel 1985). In Fig. 5 it can be seen that a more intense and narrower band characterizes samples H and I, which have small particle dimensions. In fact, SPR, which is typical of metal nanosized particles, is suppressed for larger particles, because they become more similar to the bulk state (Yeh et al. 1999; Wu et al. 2006; Slistan-Grijalvaa et al. 2005). However, SPR does not occur with very small particles, ones with a diameter below 4 nm, since the intensity of their optical band becomes low (Lisiecki and Pileni 1993; Lisiecki et al. 1996; Khanna et al. 2009).

XRD analysis showed that no oxide or organometallic compounds were formed and, even at the lowest synthesis temperature (60 °C), only metallic copper is obtained (Fig. 6a). This pattern showed peaks at 43.3 and at 50.5° 2θ, which were attributed to those of face-centered cubic metal copper (JCPDS card no. 4-0836).

Influence of the way of reagents addition

Reagent addition order

Synthesis was performed by adding the metal precursor after the reducing agent, because it was supposed that by pouring the metal salt in a strong reducing ambient a faster and more massive

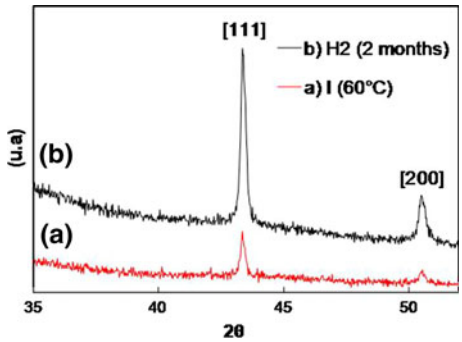

Fig. 6 XRD analysis: **a** sample I synthesized at 60 °C, **b** sample H2 (aged 2 months)

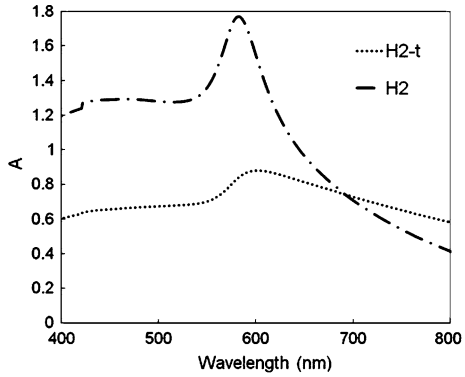

Fig. 7 Extinction band of sample H2 (microwave heating) and H2-t (traditional heating), synthesized by adding the reagents at ambient temperature

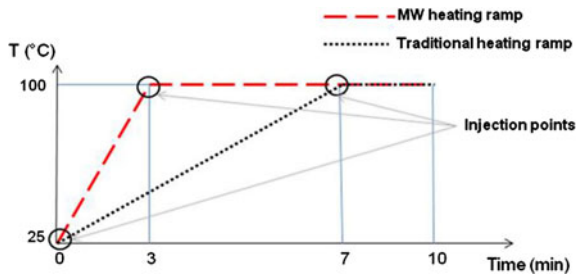

Fig. 8 Different heating ramps provided by MW and traditional heating system

nucleation would be fostered, thus avoiding an excessive particle growth. However, in order to verify this hypothesis, sample D2 was synthesized in the same way as sample D, but by reversing the reagents' order (first the metal salt and then the reducing agent). Results clearly confirmed the hypothesis, showing for the sample D2 a coarsening of particle size by DLS (Table 1), together with a red shift of the SPR band, which moved from 590 to 603 nm. Thus, the importance of tuning synthesis parameters to control nucleation and growth phenomena is stressed.

Reagent addition temperature

The reagents (reducing and metal precursor) are injected by the standard procedure only when the solution has reached the synthesis temperature, in order to maximize the nucleation rate and avoid secondary reactions during the heating ramp. Nevertheless, a process simplification, particularly for industrial scale-up, could be achieved by adding reagents at ambient temperature at the beginning of the reaction, while avoiding the injection at high temperature. In order to appraise this hypothesis, sample H2 was prepared in the same conditions as sample H, but adding reagents at ambient temperature, in order to verify the microwave effect on this procedure. Moreover, two other samples, H-t and H2-t, were obtained in the same way as samples H and H2, but by using a traditional heating system instead of a microwave (MW) device (Table 2).

Compared to sample H, the addition of reagents before microwave heating, as in sample H2, caused a slight decrease in particle size, while in sample H2-t, the same addition before traditional heating produced a massive particle growth. These phenomena are confirmed by the red shift of 20 nm in the SPR band of sample H2-t and also by its broadening (Fig. 7).

This effect can be explained by the different thermal rates provided by microwaves against traditional heating (Fig. 8): the former is so fast that even if some nuclei form during heating, they are quickly carried to the optimal temperature of 100 °C. In contrast, the latter is so slow that, if some nuclei are generated during heating, they need a long time to reach the equilibrium temperature, thus giving rise to the growth phenomena before reaching 100 °C.

Moreover, microwaves ensure homogenous heating, resulting in suspensions with a low PDI (Table 2). In addition, by periodic measurement of particle size during a 40-day storage, an instability index, expressed as nm per day, was determined for each sample. The best stability in nanoparticle size was achieved by both microwave heating and adding

metal salt and ascorbic acid at the beginning of the reaction (sample H2). When the reagents are absent during the heating ramp, as in sample H, the dielectric heating probably induced some degradation phenomena on the chelating agent, by limiting its protective function during the storage time. Therefore, the injection of reagents before microwave heating is the optimal procedure.

Similarly, the sample achieved by adding the reagents before traditional heating (H2-t) shows a lower instability index than sample H-t. Nevertheless, in this case the difference between indexes is smaller than that of samples synthesized by microwave heating, probably because during the traditional heating ramp a lower degradation of the chelating agent occurs. H2-t presents coarser particle dimensions and seems to be less exposed to aggregation. As a consequence, unlike with the microwave method, for traditional heating the optimum synthesis strategy proved to be the hot injection of metal salt in a strongly reducing ambient.

For the optimized sample H2, the XRD pattern remained unchanged after 2 months (Fig. 6b), thus indicating that the PVP coating, together with the action of the antioxidant ascorbic acid, prevents the Cu nanoparticles from oxidation, even if nanosuspensions are exposed to air.

Scanning transmission electron microscopy analysis performed on sample H2 (Fig. 9a) shows a homogeneous particle size distribution, confirming the low PDI value assessed by DLS, with a mean size of 46 nm and a standard deviation of 9 nm; the size distribution calculated by the image analysis is shown in Fig. 9b. As reported elsewhere (Altincekic and Boz 2008; Lee et al. 2008; Mullaugh and Luther 2010; Murdock et al. 2008; Tso et al. 2010), microscope analysis may deviate so much from the DLS value for various reasons. First, the laser scattering technique measures the hydrodynamic diameter comprehensive of PVP and coordinated molecules. In order to show that the hydrodynamic diameter of synthesized samples may differ so much from STEM analysis, a measure of a DEG solution containing only PVP (in the same amount as sample H2) was performed. PVP solution provides a DLS signal (graph not shown) with two peaks at different sizes (at 10 and 56 nm). Moreover, by adding ascorbic acid (in the same amount as sample H2), the size distribution changes and the second peak

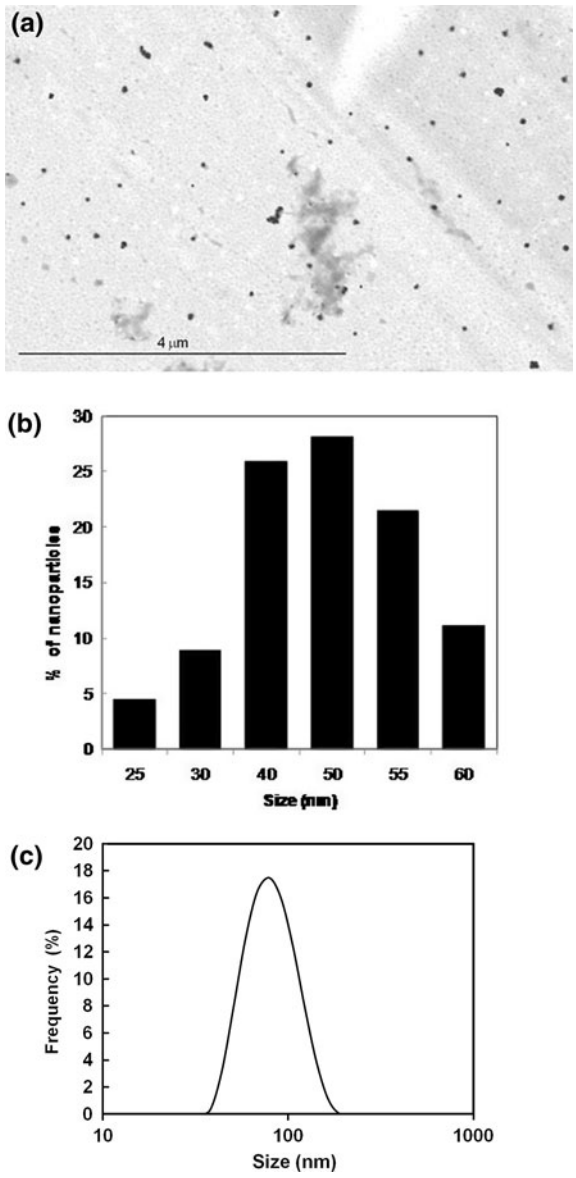

Fig. 9 **a** STEM image of sample H2, synthesized with $[Cu^{2+}] = 16.6$ mM, $[n\text{PVP}/n\text{Cu}^{2+}] = 5$, $[n\text{C}_6\text{H}_8\text{O}_6/n\text{Cu(ac)}_2] = 2.5$, $T = 100$ °C, $t = 10$ min. **b** Particle size distribution calculated by STEM analysis, average diameter: 46 nm, standard deviation: 9 nm. **c** Particle size distribution obtained by DLS analysis on sample H2, average diameter: 84 nm, standard deviation: 1 nm, PDI = 0.08

shifts to a coarse size (acid and PVP probably interact with each other, thus inducing a rearrangement of the polymer). Probably after the nucleation of nanoparticles the polymer conformation rearranges, so, due to the complexity of the system, the signal observed with only PVP and ascorbic acid cannot be subtracted

automatically from the hydrodynamic diameter of sample H2. Furthermore, since dispersed particles can aggregate locally, the coarsest sizes in the DLS distribution consist of agglomerates which strongly influence the mean size, which becomes greater than the average primary particle size calculated from the STEM image.

Optical properties and particle size correlation

A correlation between SPR band sharpness and mean particle size measured by DLS is clearly observed (Fig. 10a): the coarser the particles, the weaker the intensity of bands. This trend can be explained because SPR, typical of nanosized metal particles, is attenuated once their dimension becomes more similar to the bulk state (Yeh et al. 1999; Khanna et al. 2009). In addition, a coarser size brings about a smaller particle number per unit volume, thus resulting in a decreased SPR band intensity (Lisiecki and Pileni 1993). A linear correlation is appreciable between particle mean diameter and SPR band area, corresponding to the concentrations of two metal ions: 16.6 and 33.2 mM. Since the high metal content caused an increase in particle mean diameter, absorption band properties also changed in a different way for the two concentrations: for the same area there are two different diameters. This can be explained by the fact that, while DLS gives an average among all particles in the 1–6000 nm range, SPR revealed by UV–Vis absorbance is strictly dependent on the nanometric fraction of particles. Thus, in a sample with a high mean diameter, only small particles can contribute to the absorbance peak, behaving, in terms of the absorption peak area, as a sample with smaller mean size. Furthermore, a red shift of SPR bands is observed for particle increase (Fig. 10b): data show two linear trends between wavelength of maximum absorption and mean particle diameter, corresponding to the concentrations of two metal ions. Since the particle size resulting from DLS measurements does not refer to the metal particle diameter, but to the hydrodynamic one, the correlation is not perfectly linear. However, a higher slope can be observed for the low solid content, thus highlighting again the fact that SPR absorption is more sensitive to small mean particle size.

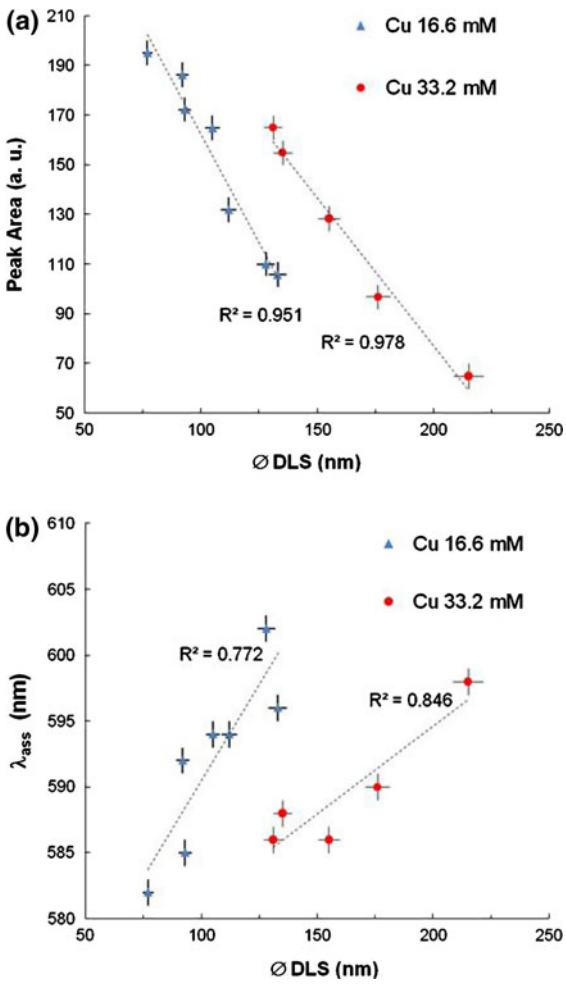

Fig. 10 Correlation between **a** mean particle size by DLS and SPR band areas, **b** mean particle size by DLS and wavelength of maximum absorption

Conclusions

Stable Cu nanosuspensions have been obtained by an environment-friendly, microwave-assisted polyol synthesis, which can be scaled up for industrial large-scale production.

The control over particle nucleation and growth has been achieved by optimization of the reducing agent content, synthesis temperature, reaction yield, and the manner of injecting the reagents; therefore, thanks to the microwave heating effect, there proved to be a crucial improvement in terms of suspension stability over time and process simplification. As a result of this optimization, stable nanosuspensions with a high solid concentration were obtained and

their stability was improved, not only avoiding precipitation for a period longer than 2 months, but also reducing the particle growth during storage; moreover, the optimized process made it possible to avoid the injection of reagents at high temperatures.

The so-prepared suspensions are totally made up of copper particles with a mean diameter of 46 ± 9 nm, calculated by STEM analysis, and a narrow size distribution also confirmed by DLS measurements.

Optical properties of copper nanoparticles depend on a 580–600 nm SPR band; a red shift was observed for coarser dimensions, together with a linear correlation between band sharpness and mean particle diameter; however, peak intensity is selectively affected by the smallest particle sizes, so that a mixture of small and coarse particles may have better properties than particles with an intermediate diameter.

Acknowledgments The authors would like to thank Dr. Andrea Barzanti and Dr. Giada Lorenzi for the electron microscope analysis of the samples.

References

Altincekic TG, Boz I (2008) Influence of synthesis conditions on particle morphology of nanosized Cu/ZnO powder by polyol method. Bull Mater Sci 31:619–624. doi:10.1007/s12034-008-0098-x

Cha SI, Mo CB, Kim KT, Jeong YJ, Honga SH (2006) Mechanism for controlling the shape of Cu nanocrystals prepared by the polyol process. J Mater Res 21:2371–2378. doi:10.1557/JMR.2006.0285

Chakroune N, Viau G, Ricolleau C, Fièvet-Vincent F, Fievet F (2003) Cobalt-based anisotropic particles prepared by the polyol process. J Mater Chem 13:312–318. doi:10.1039/b209383a

Creighton JA, Eadont DG (1991) Ultraviolet–visible absorption spectra of the colloidal metallic element. J Chem Soc Faraday Trans 87:3881. doi:10.1039/FT9918703881

Daungthongsuk W, Wongwises S (2007) A critical review of convective heat transfer of nanofluids. Renew Sustain Energy Rev 11:797–817. doi:10.1016/j.rser.2005.06.005

Dotzauer DM, Bhattacharjee S, Wen Y, Bruening ML (2009) Nanoparticle-containing membranes for the catalytic reduction of nitroaromatic compounds. Langmuir 25:1865–1871. doi:10.1021/la803220z

Feldmann C, Jungk HO (2001) Polyol-mediated preparation of nanoscale oxide particles. Angew Chem Int Ed 40:359–362. doi:10.1002/1521-3773(20010119)40:2<359:AID-ANIE359>3.0.CO;2-B

Feldmann C, Jungk HO (2002) Preparation of sub-micrometer $LnPO_4$ particles (Ln = La, Ce). J Mater Sci 37:3251–3254. doi:10.1023/A:1016131016637

Fievet F (2000) Polyol process. In: Sugimoto T (ed) Fine particles: synthesis, characterization, and mechanism of growth. Surfactant science series, vol 92. M. Dekker, Inc., New York, p 460

Fievet F, Fievet VF, Lagier JP, Dumont B, Figlarz M (1993) Controlled nucleation and growth of micrometre-size copper particles prepared by the polyol process. J Mater Chem 3:627–632. doi:10.1039/JM9930300627

Gritaonandia JS et al (2008) Chemically induced permanent magnetism in Au, Ag, and Cu nanoparticles: localization of the magnetism by element selective techniques. Nano Lett 8:661–667. doi:10.1021/nl073129g

Hammarberg E, Prodi Shwab A, Feldmann C (2009) Microwave-assisted polyol synthesis of aluminium- and indium-doped ZnO nanocrystals. J Colloid Interface Sci 334:29–36. doi:10.1016/j.jcis.2009.03.010

Haq S, Raval R (2007) NO and dichloroethene reactivity on single crystal and supported Cu nanoparticles: just how big is the materials gap? Phys Chem Chem Phys 9:3641–3647. doi:10.1039/b702595p

Huang H et al (1997) Synthesis, characterization and nonlinear optical properties of copper nanoparticles. Langmuir 13:172–175. doi:10.1021/la9605495

Hutter E, Fendler JH (2004) Exploitation of localized surface plasmon resonance. Adv Mater 16:1685–1706. doi:10.1002/adma.200400271

Khanna PK, More P, Jawalkar J, Patil Y, Rao NK (2009) Synthesis of hydrophilic copper nanoparticles: effect of reaction temperature. J Nanopart Res 11:793–799. doi:10.1007/s11051-008-9441-9

Kim YH, Lee DK, Cha HG, Kim CW, Kang YC, Kang YS (2006a) Preparation and characterization of the antibacterial Cu nanoparticle formed on the surface of SiO_2 nanoparticles. J Phys Chem B 110:24923–24928. doi:10.1021/jp0656779

Kim YH, Lee DK, Jo BG, Jeong JH, Kang YS (2006b) Synthesis of oleate capped Cu nanoparticles by thermal decomposition. Colloid Surf A Physiochem Eng Aspects 284–285:364–368. doi:10.1016/j.colsurfa.2005.10.067

Kobayashi Y, Ishida S, Ihara K, Yasuda Y, Morita T, Yamada S (2009) Synthesis of metallic copper nanoparticles coated with polypyrrole. Colloid Polym Sci 287:877–880. doi:10.1007/s00396-009-2047-7

Kreibig U, Genzel L (1985) Optical absorption of small metallic particles. Surf Sci 156:678–700. doi:10.1134/1.558284

LaMer V, Dinegar R (1950) Theory, production and mechanism of formation of monodispersed hydrosols. J Am Chem Soc 72:4847–4854. doi:10.1021/ja01167a001

Lee Y, Choi J, Lee KJ, Stott NE, Kimet D (2008) Large-scale synthesis of copper nanoparticles by chemically controlled reduction for applications of inkjet-printed electronics. Nanotechnology 19:415604. doi:10.1088/0957-4484/19/41/415604

Lisiecki I, Pileni MP (1993) Synthesis of copper metallic clusters using reverse micelles as microreactors. J Am Chem Soc 115:3887–3896. doi:10.1021/ja00063a006

Lisiecki I, Billoudet F, Pileni MP (1996) Control of the shape and the size of copper metallic particles. J Phys Chem 100:4160–4166. doi:10.1021/jp9523837

Liu Z, Bando Y (2003) A novel method for preparing copper nanorods and nanowires. Adv Mater 15:303–305. doi:10.1002/adma.200390073

Liu MS, Lin MCC, Tsai CY, Wang CC (2006) Enhancement of thermal conductivity with Cu for nanofluids using chemical reduction method. Int J Heat Mass Transf 49:3028–3033. doi:10.1016/j.ijheatmasstransfer.2006.02.012

Liu YH, Lo SL, Lin CJ (2007) Size effect in reactivity of copper nanoparticles to carbon tetrachloride degradation. Water Res 41:1705–1712. doi:10.1016/j.watres.2007.01.014

Lu X, Rycenga M, Skrabalak SE, Wiley B, Xia Y (2009) Chemical synthesis of novel plasmonic nanoparticles. Annu Rev Phys Chem 60:167–192. doi:10.1146/annurev.physchem.040808.090434

Mullaugh KM, Luther GW (2010) Spectroscopic determination of the size of cadmium sulfide nanoparticles. J Environ Monit 12:890–897. doi:10.1039/b919917a

Murdock RC et al (2008) Characterization of nanomaterial dispersion in solution prior to in vitro exposure using dynamic light scattering technique. Toxicol Sci 101:239–253. doi:10.1093/toxsci/kfm240

Nada EA, Masoud Z, Hijazi A (2008) Natural convection heat transfer enhancement in horizontal concentric annuli using nanofluids. Int Commun Heat Mass Tranf 35:657–665. doi:10.1016/j.icheatmasstransfer.2007.11.004

Nakamura T, Tsukahara Y, Sakata T, Mori H, Kanbe Y, Bessho H, Wada Y (2007) Preparation of monodispersed Cu nanoparticles by microwave-assisted alcohol reduction. Bull Chem Soc Jpn 80:224–232. doi:10.1246/bcsj.80.224

Park BK, Jeong S, Kim D, Moon J, Lim S, Kim JS (2007) Synthesis and size control of monodisperse copper nanoparticles by polyol method. J Colloid Interface Sci 311:417–424. doi:10.1016/j.jcis.2007.03.03

Ren X, Chen D, Tang F (2005) Shape-controlled synthesis of copper colloids with a simple chemical route. J Phys Chem B 109:15803–15807. doi:10.1021/jp052374q

Sarkar A, Mukherjee T, Kapoor SJ (2008) PVP-stabilized copper nanoparticles: a reusable catalyst for "click" reaction between terminal alkynes and azides in non-aqueous solvents. J Phys Chem C 113:3334–3340. doi:10.1021/jp077603i

Sidorov SN, Bronstein LM, Valetsky PM, Hartmann J, Colfen H, Schnablegger H, Antonietti M (1999) Stabilization of metal nanoparticles in aqueous medium by polyethyleneoxide–polyethyleneimine block copolymers. J Colloid Interface Sci 212:197–211. doi:10.1006/jcis.1998.6035

Singh AK, Raykar VS (2008) Microwave synthesis of silver nanofluids with polyvinylpyrrolidone (PVP) and their transport properties. Colloid Polym Sci 286:1667–1673. doi:10.1007/s00396-008-1932-9

Slistan-Grijalvaa A, Herrera-Urbina R, Rivas-Silva JF, Valos-Borja MA, Castillon-Barraza FF, Posada-Amarillas A (2005) Classical theoretical characterization of the surface plasmon absorption band for silver spherical nanoparticles suspended in water and ethylene glycol. Physica E 27:104–112. doi:10.1016/j.physe.2004.10.014

Son SU, Park IK, Park J, Hyeon T (2004) Synthesis of Cu_2O coated Cu nanoparticles and their successful applications to Ullmann-type amination coupling reactions of aryl chlorides. Chem Commun 7:778–779. doi:10.1039/b316147a

Sun J, Jing Y, Jia Y, Tillard M, Belin C (2005) Mechanism of preparing ultrafine copper powder by polyol process. Mater Lett 59:3933–3936. doi:10.1016/j.matlet.2005.07.036

Tanabe K (2007) Optical radiation efficiencies of metal nanoparticles for optoelectronic applications. Mater Lett 61:4573–4575. doi:10.1016/j.matlet.2007.02.053

Tso C, Zhung C, Shih Y, Tseng YM, Wu S, Doonget R (2010) Stability of metal oxide nanoparticles in aqueous solutions. Water Sci Technol 61:127–133. doi:10.1016/j.watres.2007.11.036

Viau G, Toneguzzo P, Perrard A, Acher O, Fièvet-Vincent F, Fievet F (2001) Heterogeneous nucleation and growth of metal nanoparticles in polyols. Scr Mater 44:2263–2267. doi:10.1016/S1359-6462(01)00752-7

Wang Y, Chen P, Liu M (2006) Synthesis of well-defined copper nanocubes by a one-pot solution process. Nanotechnology 17:6000–6006. doi:10.1088/0957-4484/17/24/016

Wu SH, Chen DH (2004) Synthesis of high-concentration Cu nanoparticles in aqueous CTAB solutions. J Colloid Interface Sci 273:165–169. doi:10.1016/j.jcis.2004.01.071

Wu C, Mosher BP, Zeng T (2006) One-step green route to narrowly dispersed copper nanocrystals. J Nanopart Res 8:965–969. doi:10.1007/s11051-005-9065-2

Yang J, Okamoto T, Ichino R, Bessho T, Satake S, Okido M (2006) A simple way for preparing antioxidation nano-copper powders. Chem Lett 35:648–649. doi:10.1246/cl.2006.648

Yeh MS, Yang YS, Lee YP, Lee HF, Yeh YH, Yeh CS (1999) Formation and characteristics of Cu colloids from CuO powder by laser Irradiation in 2-propanol. J Phys Chem B 103:6851–6857. doi:10.1021/jp984163+

Yu W, France DM, Routbort JL, Choi US (2008) Review and comparison of nanofluid thermal conductivity and heat transfer enhancements. Heat Transf Eng 29:432–460. doi:10.1080/01457630701850851

Zhao Y, Zhu JJ, Hong JM, Bian N, Chen HY (2004) Microwave-induced polyol-process synthesis of copper and copper oxide nanocrystals with controllable morphology. Eur J Inorg Chem 2004:4072–4080. doi:10.1002/ejic.200400258

Zheng J, Nicovich PR, Dickson RM (2007) Highly fluorescent noble-metal quantum dots. Annu Rev Phys Chem 58:409–431. doi:10.1146/annurev.physchem.58.032806.104546

Zhu J, Li K, Chen H, Yang X, Lu L, Wang X (2004a) Highly dispersed CuO nanoparticles prepared by a novel quick-precipitation method. Mater Lett 58:3324–3327. doi:10.1016/j.matlet.2004.06.031

Zhu HT, Zhang C, Yin Y (2004b) Rapid synthesis of copper nanoparticles by sodium hypophosphite reduction in ethylene glycol under microwave irradiation. J Cryst Growth 270:722–728. doi:10.1016/j.jcrysgro.2004.07.008

Zhu H, Zhang C, Yin Y (2005) Novel synthesis of copper nanoparticles: influence of the synthesis conditions on the particle size. Nanotechnology 16:3079–3083. doi:10.1088/0957-4484/16/12/059